Research Article

Journal of PeptideScience

Received: 15 July 2010 Revised: 16 August 2010 Accepted: 24 August 2010 Published online in Wiley Online Library: 26 October 2010

(wileyonlinelibrary.com) DOI 10.1002/psc.1304

Rational design of peptide nanotubes for varying diameters and lengths‡

Motoki Ueda,[a] Akira Makino,[a] Tomoya Imai,[b] Junji Sugiyama[b] and Shunsaku Kimura[a]*

Amphiphilic helical peptides $(Sar)_m$-*b*-(L-Leu-Aib)$_n$ (m = 22–25; n = 7, 8, 10) with a hydrophobic block as a right-handed helix were synthesized and their mixtures with $(Sar)_{25}$-*b*-(D-Leu-Aib)$_6$ containing the hydrophobic block as a left-handed helix were examined in their molecular assembly formation. The single component $(Sar)_{25}$-*b*-(D-Leu-Aib)$_6$ forms peptide nanotubes of 70 nm diameter and 200 nm length. The two-component mixtures of $(Sar)_{25}$-*b*-(D-Leu-Aib)$_6$ with $(Sar)_{24}$-*b*-(L-Leu-Aib)$_7$, $(Sar)_{22}$-*b*-(L-Leu-Aib)$_8$, and $(Sar)_{25}$-*b*-(L-Leu-Aib)$_{10}$ yield peptide nanotubes of varying dimensions with 200 nm diameter and 400 nm length, 70 nm diameter and several micrometer length (maximum 30 μm), and 70 nm diameter and 100–600 nm length, respectively. The right-handed and the left-handed helix were thus found to be molecularly mixed due to the stereo-complex formation and to generate nanotubes of different sizes. When the mismatch of the hydrophobic helical length between the two components was of four residues, the longest nanotube was generated. Correspondingly, the hydrophobic helical segments have to interdigitate with an anti-parallel orientation at the hydrophobic core region of the nanotube. Copyright © 2010 European Peptide Society and John Wiley & Sons, Ltd.

Supporting information may be found in the online version of this article

Keywords: amphiphiles; block copolymers; nanotubes; polypeptides; self-assembly

Introduction

Precise control of morphology is an important challenge in the field of molecular self-assembly [1–4]. Nano-ordered tubular assemblies, nanotubes, are of interest due to their numerous possible applications. For example, hollow tubular structures provide closed reaction chambers when adjusting the space to guest molecules as demonstrated by protein-folding chaperonins [5,6] and protein-degradation enzymes [7]. Peptide amphiphiles have been used for the preparation of molecular assemblies in a wide range of morphologies such as micelles [8], cylinder micelles [9], fibres [10], nanotubes [11,12], and vesicles [13]. We have reported that amphiphilic peptides, especially composed of hydrophobic helical peptides, form vesicles (named peptosomes) and nanotubes characterized uniquely by their narrow size distribution [14–19]. Indeed helical peptides have the ability to pack in regular mode in molecular assemblies as shown by frequent occurrence of helix bundles in proteins [20,21].

$(Sar)_{27}$-*b*-(L-Leu-Aib)$_6$, an amphiphilic helical peptide, was found to form peptide nanotubes with a diameter of about 70 nm and a length of about 200 nm [14]. The self-assembling process is constituted of two steps. Initially, the amphiphilic helical peptide forms a curved square sheet assembly upon dispersion in buffer at room temperature. Heating the dispersion at 90 °C for 10 min triggers the morphological conversion from the curved sheet to nanotube. The length of the nanotube is further increased by additional heating for 24 h to reach about 1 μm; however, it is difficult to obtain very long nanotubes of an aspect ratio more than 100. For the preparation of the longer peptide nanotubes, nanotubes with more robust membranes are required.

In the present study, the effect of stereo-complexes on helix association in molecular assemblies was examined. A typical example of stereo-complex formation was reported between the right-handed and the left-handed helices of poly-(lactic acid)$_n$. The stereo-mixture was found to possess improved properties in terms of mechanical strength and heat resistance than each enantiomer [22,23]. Correspondingly, a mixture of right-handed and left-handed helical peptides is expected to form a stereo-complex as a result of the convex–concave complementarity of their surfaces. In this report, we demonstrate that indeed robust and long nanotubes are obtained as a result of the stereo-complex formation between right- and left-handed helices differing in their helix lengths.

* *Correspondence to: Shunsaku Kimura, Department of Material Chemistry, Graduate School of Engineering, Kyoto University, Kyoto-Daigaku-Katsura, Nishikyo-ku, Kyoto 615-8510, Japan. E-mail: shun@scl.kyoto-u.ac.jp*

a *Department of Material Chemistry, Graduate School of Engineering, Kyoto University, Kyoto-Daigaku-Katsura, Nishikyo-ku, Kyoto 615-8510, Japan*

b *Research Institute for Sustainable Humanosphere (RISH), Kyoto University, Gokasho, Uji, Kyoto 611-0011, Japan*

‡ *Special issue devoted to contributions presented at the E-MRS Symposium C "Peptide-based materials: from nanostructures to applications", 7-11 June 2010, Strasbourg, France.*

Journal of PeptideScience

Materials and Methods

Peptides

The peptides were synthesized by conventional procedures in solution following essentially protocols reported previously [14]. The hydrophobic helical segments (D-Leu-Aib)$_6$ and (L-Leu-Aib)$_m$ (m = 7, 8, 10) were prepared by fragment condensation, whereas the poly-sarcosine extension at the *N*-termini of the helical segments was obtained by the NCA (*N*-carboxy anhydride) polymerization. MALDI-TOF MS analysis and the area ratios of Sar N-CH_3 peaks against those of OCH_3 of the *C*-termini in ^{1}H-NMR spectra were used to determine the degrees of polymerization of 24, 22, and 25, respectively (Figure S1, Supporting Information).

Preparation of Molecular Assemblies

Equimolar mixtures of two polypeptides (1 μmol each) were dissolved in ethanol (40 μl) and injected into a buffer (1 ml, 10 mM Tris–HCl, pH 7.4) under stirring at 4 °C. After 30 min, the dispersions were heated at 90 °C for a specified period.

Circular Dichroism

Circular Dichroism (CD) measurements were carried out on a JASCO J600 spectropolarimeter with a quartz cell of 0.1 cm optical path length at room temperature. The sample concentration in 10 mM Tris–HCl buffer (pH 7.4) was 0.375 mM (per amino acid residue).

Transmission Electron Microscopy

Transmission Electron Microscopy (TEM) images were taken by using a JEOL JEM-2000EXII at an accelerating voltage of 100 kV. For the observation, a drop of dispersion was mounted on a carbon-coated Cu grid and stained negatively with 2% uranyl acetate, followed by suction of the excess fluid with a filter paper.

Results and Discussion

Poly(sarcosine) (poly(Sar)) was used in the present work as the hydrophilic block, as its hydrophilicity is similar to that of poly(ethylene glycol). Moreover, Sar is biocompatible due to its biodegradability *in vivo* by endogenous Sar dehydrogenase. We have previously applied the amphiphilic peptide micelles of (Sar)$_n$-*b*-(Glu-OMe)$_m$ [15] or (Sar)$_n$-*b*-(Lac)$_m$ (Lac represents L-lactic acid) [16] with near-infrared fluorescence probes for *in vivo* tumour imaging. These poly(Sar) conjugates were shown to be highly biocompatible.

The hydrophilic block of (Sar)$_n$ was attached to the *N*-termini of the hydrophobic helical blocks of (D-Leu-Aib)$_6$ and (L-Leu-Aib)$_m$ (m = 7, 8 and 10) via polymerization of Sar NCA to obtain **S25D12, S24L14, S22L16**, and **S25L20** (Figure 1), respectively. Similar sizes of the Sar block were adopted to avoid the complexity of molecular parameters inducing morphology change. CD spectra of each peptide in buffer after heat treatment at 90 °C for 24 h indicated, as expected, the presence of a left-handed α-helix for **S25D12** and right-handed α-helices for **S24L14, S22L16**, and **S25L20** (Figure S2).

The morphology of the molecular assemblies of mixtures of two components after heat treatment at 90 °C for 24 h was analysed by TEM with negative staining. One component of the peptide mixture was the **S25D12** with its left-handed α-helix. As second component, **S24L14, S22L16**, and **S25L20** were added with their right-handed α-helices of different lengths. In the case of the equimolar mixture of **S25D12** and **S24L14** (**DL14**), nanotubes of 200 nm diameter and 400 nm length and elliptical planar sheets of 200–300 nm were obtained (Figures 2a and 4). On the other hand, the mixture of **S25D12** and **S22L16** (**DL16**) yields long nanotubes of 70 nm diameter and 2–30 μm length and planar sheets of 50–200 nm (Figures 2b and 4), whereby single- and multi-walled long nanotubes of **DL16** were detected (Figure 2d and 2e). A mixture of **S25D12** with the longest right-handed α-helix **S25L20** (**DL20**) led to the formation of short nanotubes with 70 nm diameter and 100–600 nm length as well as twisted

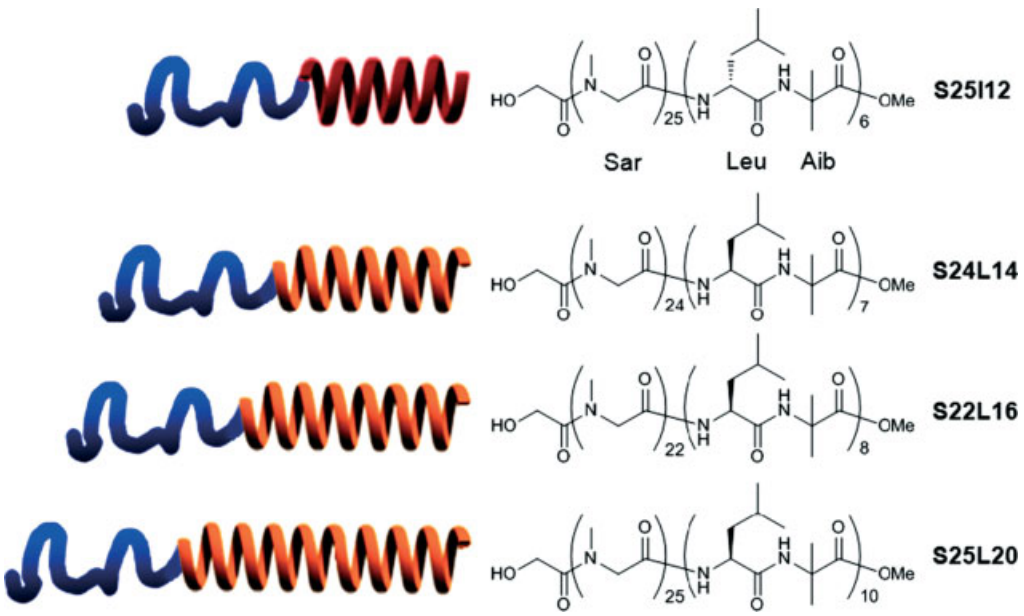

Figure 1. Molecular structure of the amphiphilic polypeptides. The (Sar)$_m$ constitutes the unstructured hydrophilic block and (Leu-Aib)$_n$ the hydrophobic α-helical block.

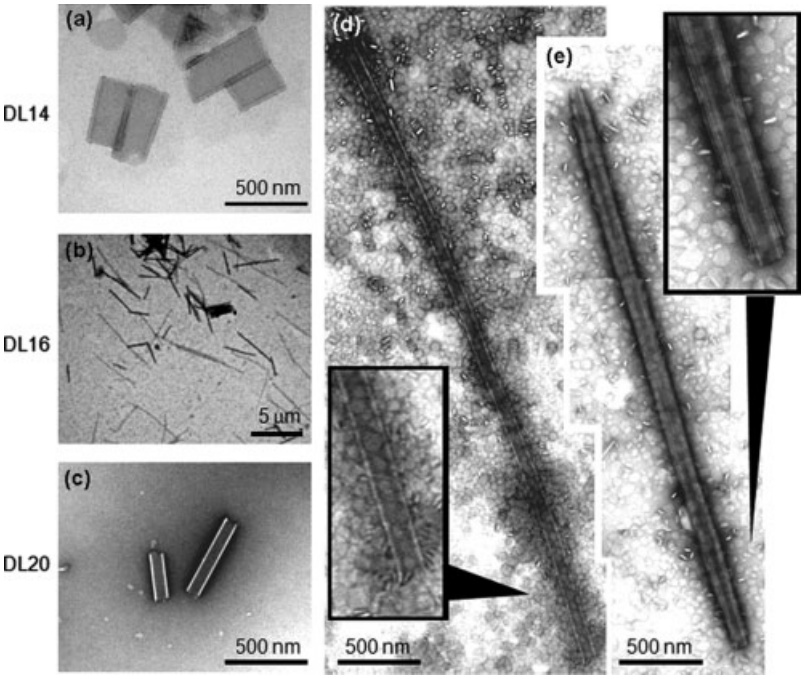

Figure 2. TEM images (negative staining with uranyl acetate (a–e) of molecular assemblies from equimolar mixtures of helical polypeptides **S25D12** and **S24L14** (a); **S25D12** and **S22L16** (b, d, e); **S25D12** and **S25L20** (c). The assemblies were prepared in 10 mM Tris–HCl buffer (pH 7.4) (2 μmol/1 ml) by the ethanol injection method and heat treatment. (d) and (e) show the magnified view of (b).

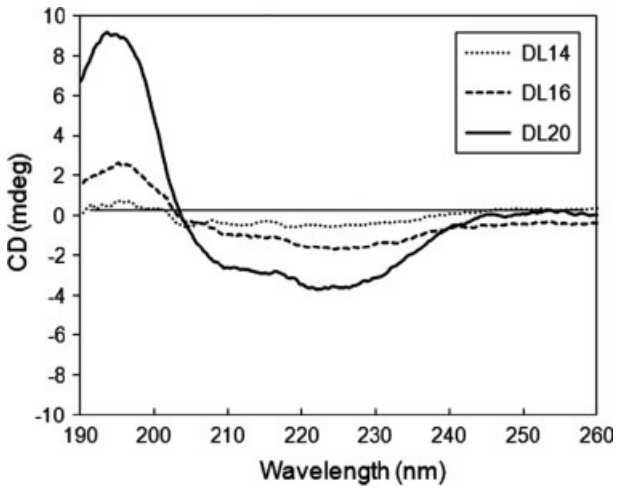

Figure 3. CD spectra of assemblies from **DL14** (dot line), **DL16** (dash line), and **DL20** (solid line) in Tris buffer after heating at 90 °C for 24 h and purification through a Sephacryl S-100 column. The increased ratio of the intensity at 222 nm compared to that at 208 nm indicates a helix bundle structure.

ribbons of 300 nm (Figures 2c and 4). No multi-walled nanotubes were found in the cases of **DL14** and **DL20**.

In the first instance, the question was examined whether the nanotubes observed in these mixtures were indeed consisting of the two components. For this purpose, the assembly dispersions of **DL14,DL16**, and **DL20** were purified by a Sephacryl S-100 column to obtain fractions including the dominant nanotubes. CD spectra of these fractions show negative Cotton effects with intensities that are smaller than those of the molecular assemblies prepared from the corresponding single components **S24L14, S22L16**, and **S25L20** (Figure 3 and S2). The reduced intensities can be attributed to the coexistence of **S25D12** in the nanotubes. Indeed, the residual intensities increase in the order of **DL14** < **DL16** < **DL20**, which corresponds to the order of the helix-length difference of **S24L14** < **S22L16** < **S25L20** from **S25D12**. The molar ratios of the left- and the right-handed helix in the nanotubes as estimated from the intensities of the Cotton effects are 1/0.97 for **S25D12**/**S24L14**, 1/0.95 for **S25D12**/**S22L16** and 1/0.93 for **S25D12**/**S25L20**, confirming that the nanotubes are composed of equimolar mixtures of the peptides. Furthermore, the increased ratio of the intensity at 222 nm compared to that at 208 nm indicates a helix bundle structure, which results from the strong association of neighbouring helices [24].

Additionally, TEM observations of the molecular assemblies prepared from the single components of **S25D12, S24L14, S22L16**, and **S25L20**, support the coexistence of the two peptides in the nanotubes of **DL14, DL16**, and **DL20**. In fact, TEM images show that **S25D12** and **S24L14** form in the buffer nanotubes of 70 nm diameter and 200 nm length, whereas **S22L16** yields vesicles of 100 nm diameter, and **S25L20**, small planar sheets (Figure S5), which are different from the nanotubes obtained from **DL14, DL16**, and **DL20**.

The membrane thicknesses of the assemblies prepared from **DL14, DL16**, and **DL20** were of about 10 nm. In the membranes, the helices are supposed to be aligned in an interdigitated manner with anti-parallel orientation to gain the favourable dipole–dipole stabilization between peptide helices. As the hydrophobic helical peptide has 2–3 nm chain length, the sarcosine chain length should be 7–8 nm in the assembly, suggesting a moderately extended conformation of the poly(Sar) chain in the membrane. The ^{1}H-NMR spectra of **S25D12, S24L14, S22L16**, and **S25L20** in methanol showed two kinds of N–CH_3 signals due to the coexistence of the *cis* and *trans* configurations of sarcosine amides (data not shown), indicating that the poly(Sar) chains are flexible [25,26].

Journal of PeptideScience

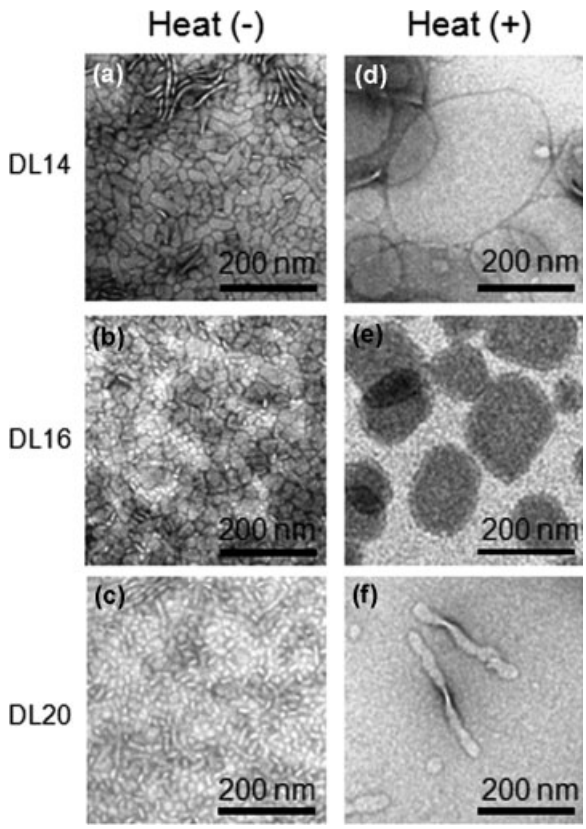

Figure 4. TEM images of each sheet structure of **DL14** (a and d), **DL16** (b and e), and **DL20** (c and f). The assemblies were prepared in 10 mM Tris–HCl buffer (pH 7.4) (2 μmol/1 ml) by the ethanol injection method. Before heat treatment (a–c) and after heat treatment at 90 °C for 24 h (d–f).

The diameter of the nanotubes in the case of **DL14** is the largest among the present combinations of two kinds of peptides. **S25D12** alone forms a curved sheet before heat treatment in the preparation of the molecular assembly, because the left-handed helices should be molecularly packed in a consecutive twisted manner with a defined tilt angle between the helices as demonstrated by cholesteric liquid crystals of helical compounds. Upon mixing the left- and the right-handed helices, the twisting property should be lost in the molecular assembly, resulting in a smaller curvature of the nanotube of **DL14** than that of **S25D12**. However, there is a mismatch of the helix lengths by two residues between **S25D12** and **S24L14**, which leads to the curvature of the molecular assembly because of the excess helicity in the hydrophobic core. This is the reason why **DL14** yields thick nanotubes of moderate curvature.

On the other hand, in the cases of **DL16** and **DL20**, the mismatch lengths are four residues (6 Å) and eight residues (12 Å), respectively, which should cause a large curvature of the nanotubes. However, **DL16** yielded the long nanotubes of about 10 μm in contrast to the short nanotubes of **DL20**. To better understand the differences in the morphologies on the molecular basis, the process of formation of these molecular assemblies were analysed by TEM measurements before and after heat treatment.

In the case of **DL14**, planar elliptical sheets of 20 nm minor axis and 100 nm major axis are formed before heat treatment (Figure 4a). Upon heat treatment at 90 °C for 24 h, the planar sheets grow up to the large elliptical sheets of 200 nm minor axis and 400 nm major axis (Figure 4d). In these TEM images, many structures under transformation from planar sheets to nanotubes are also observed (Figure 5a–f). The nanotube formation is thus explained as follows. The large elliptical sheets are rolled up, and the opposite hydrophobic edges stick together to form nanotubes followed by rearrangement at the open mouth of the nanotubes from ragged ends to blunt ends. The resulting nanotube length is relatively uniform (Figure S3), because the nanotube is formed directly from a planar sheet, size of which is determined by the growth conditions of 90 °C for 24 h. No further nanotube elongation has taken place.

In the case of **DL16**, planar rectangular sheets with sides of 30 and 50 nm are observed before heat treatment (Figure 4b). Upon heat treatment at 90 °C for 24 h, the planar sheets also grow up to the moderate size of rectangular sheets with sides of 150 and 200 nm; however, no large sheets are formed (Figure 4e). In the same TEM images, nanotubes of 70 nm diameter and 200 nm length as well as the long nanotubes are identified (Figure 5g and h). The long nanotubes are thus formed by continuous attachment of the sheets to the open mouth of the nanotube, which are then rolled up to form the elongated nanotubes with ragged ends (Figures 5i and S6). The wide distribution in nanotube lengths can also be accounted for by this mechanism (Figure S3).

In the case of **DL20**, micelles of about 20 nm and nanotubes of 70 nm diameter and 100 nm length coexist before heating (Figure 4c). Upon heat treatment at 90 °C for 24 h, the twist ribbons and the nanotubes of 70 nm diameter and 100–600 nm length are formed (Figure 4f). As the open mouth of **DL20** nanotubes looks ragged similar to that of **DL16** nanotubes, the transformation mechanism of **DL20** is the same as that of **DL16** (Figure 5j–l). However, the large mismatch of the helix lengths in the case of **DL20** favours formation of stable twist ribbons, which hinders the elongation of nanotubes.

Conclusion

Analysis of the morphologies formed by the assembly of right- and left-handed α-helical peptides with mismatched helix lengths confirmed formation of long and straight peptide nanotube of 30 μm length and 70 nm diameter. The elongation of the peptide nanotubes became possible because of the strengthened membrane due to the stereo-complex formation of the right- and the left-handed helices. The curvature of nanotubes is affected by the degree of mismatch between the right- and the left-handed helices. Amphiphilic peptides having a hydrophilic block differing in size are also expected to affect the morphology and physical stability of the molecular assemblies. As amphiphilic helical peptides containing nearly the same hydrophilic block were used in this work, even this aspect is analysed in an ongoing study.

Acknowledgements

This study is a part of joint research, which is focusing on the development of the technological platform for establishing COE for nanomedicine. It is supported by the Kyoto City Collaboration of Regional Entities for Advancing Technology Excellence (CREATE) assigned by Japan Science and Technology Agency (JST).

Supporting information

Supporting information may be found in the online version of this article.

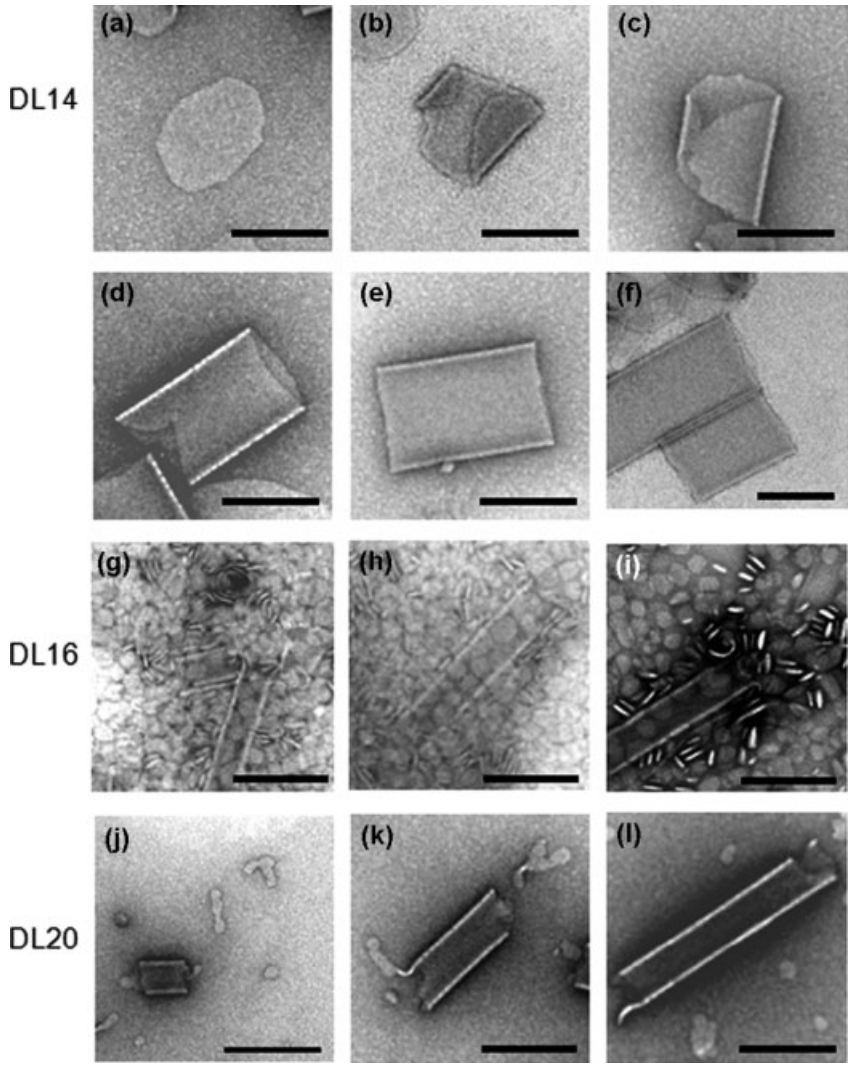

Figure 5. The formation mechanism from sheet or micelle to nanotubes of **DL14** (a–e), **DL16** (g, h), **DL20** (j, k), respectively. The magnified view of edge parts of nanotube (f, i, l). The scale bars are 200 nm for (a–h, j, k) and 100 nm for (i) and (l).

References

1 Discher DE, Eisenberg A. Polymer vesicles. *Science* 2002; **297**: 967–973.
2 Engelkamp H, Middelbeek S, Nolte RJM. Self-assembly of disk-shaped molecules to coiled-coil aggregates with tunable helicity. *Science* 1999; **284**: 785–788.
3 Jonkheijm P, van der Schoot P, Schenning APHJ, Meijer EW. Probing the solvent-assisted nucleation pathway in chemical self-assembly. *Science* 2006; **313**: 80–83.
4 Percec V, Dulcey AE, Balagurusamy VSK, Miura Y, Smidrkal J, Peterca M, Nummelin S, Edlund U, Hudson SD, Heiney PA, Duan H, Magonov SN, Vinogrado SA. Self-assembly of amphiphilic dendritic dipeptides into helical pores. *Nature* 2004; **430**: 764–768.
5 Sigler PB, Xu Z, Rye HS, Burston SG, Fenton WA, Horwich AL. Structure and function in GroEL-mediated protein folding. *Annu. Rev. Biochem.* 1998; **67**: 581–608.
6 Horwich AL, Weber-Ban EU, Finley D. Chaperone rings in protein folding and degradation. *Proc. Natl. Acad. Sci. U.S.A.* 1999; **96**: 11033–11040.
7 Voges D, Zwickl P, Baumeister W. The 26S proteasome: a molecular machine designed for controlled proteolysis. *Annu. Rev. Biochem.* 1999; **68**: 1015–1068.
8 Kim W, Thévenot J, Ibarboure E, Lecommandoux S, Chaikof E. Self-assembly of thermally responsive amphiphilic diblock copolypeptides into spherical micellar nanoparticles. *Angew. Chem. Int. Ed.* 2010; **49**: 4257–4260.
9 Zhang S. Fabrication of novel biomaterials through molecular self-assembly. *Nat. Biotechnol.* 2003; **21**: 1171–1178.
10 Cui H, Muraoka T, Cheetham AG, Stupp SI. Self-assembly of giant peptide nanobelts. *Nano Lett.* 2009; **9**: 945–951.
11 Scanlon S, Aggeli A. Self-assembling peptide nanotubes. *Nano Today* 2008; **3**: 22–30.
12 Gao X, Matsui H. Peptide-based nanotubes and their applications in bionanotechnology. *Adv. Mater.* 2005; **17**: 2037–2050.
13 Holowka EP, Sun VZ, Kamei DT, Deming TJ. Polyarginine segments in block copolypeptides drive both vesicular assembly and intracellular delivery. *Nat. Mater.* 2007; **6**: 52–57.
14 Kanzaki T, Horikawa Y, Makino A, Sugiyama J, Kimura S. Nanotube and three-way nanotube formation with nonionic amphiphilic block peptides. *Macromol. Biosci.* 2008; **8**: 1026–1033.
15 Tanisaka H, Kondoh KS, Makino A, Tanaka S, Hiraoka M, Kimura S. Near-infrared fluorescent labeled peptosome for application to cancer imaging. *Bioconjugate Chem.* 2008; **19**: 109–117.
16 Makino A, Kondoh KS, Yamahara R, Hara I, Kanzaki T, Ozeki E, Hiraoka M, Kimura S. Near-infrared fluorescence tumor imaging using nanocarrier composed of poly(L-lactic acid)-block-poly(sarcosine) amphiphilic polydepsipeptide. *Biomaterials* 2009; **30**: 5156–5160.
17 Fujita K, Kimura S, Imanishi Y. Spherical self-assembly of a synthetic α-helical peptide in water. *Langmuir* 1999; **15**: 4377–4379.

18 Kimura S, Kim D, Sugiyama J, Imanishi Y. Vesicular self-assembly of a helical peptide in water. *Langmuir* 1999; **15**: 4461–4463.
19 Kimura S, Muraji Y, Sugiyama J, Fujita K, Imanishi Y. Spontaneous vesicle formation by helical glycopeptides in water. *J. Colloid Interface Sci.* 2000; **222**: 265–267.
20 Milburn M, Prive G, Milligan D, Scott W, Yeh J, Koxhland D, Kim S. Three-dimensional structures of the ligand-binding domain of the bacterial aspartate receptor with and without a ligand. *Science* 1991; **254**: 1342–1347.
21 Parker MW, Pattus F, Tucker AD, Tsernoglou D. Structure of the membrane-pore-forming fragment of colicin A. *Nature* 1989; **337**: 93–96.
22 Fukushima K, Kimura Y. Stereocomplexed polylactides (Neo-PLA) as high-performance bio-based polymers: their formation, properties, and application. *Polym. Int.* 2006; **55**: 626–642.
23 Fukushima K, Chang Y, Kimura Y. Enhanced stereocomplex formation of poly(L-lactic acid) and poly(D-lactic acid) in the presence of stereoblock poly(lactic acid). *Macromol. Biosci.* 2007; **7**: 829–835.
24 Gibson NJ, Cassim JY. Evidence for an q-type helical conformation for bacteriorhodopsin in the purple membrane. *Biochemistry* 1989; **28**: 2134–2139.
25 Toniolo C, Bonora GM, Schilling FC, Bovey FA. Proton magnetic resonance study of linear sarcosine oligomer. *Macromolecules* 1980; **13**: 1381–1395.
26 Kimura S, Imanishi Y. Synthesis and conformation of cyclic hexapeptide cyclo(Pro-Sar-Sar)$_2$. *Int. J. Biol. Macromol.* 1981; **3**: 183–187.

